ACS SyntheticBiology

pubs.acs.org/synthbio

Research Article

Allosteric Regulation of DNA Circuits Enables Minimal and Rapid Biosensors of Small Molecules

Alan F. Rodríguez-Serrano and I-Ming Hsing*

Cite This: *ACS Synth. Biol.* 2021, 10, 371−378

Read Online

ACCESS | Metrics & More | Article Recommendations | Supporting Information

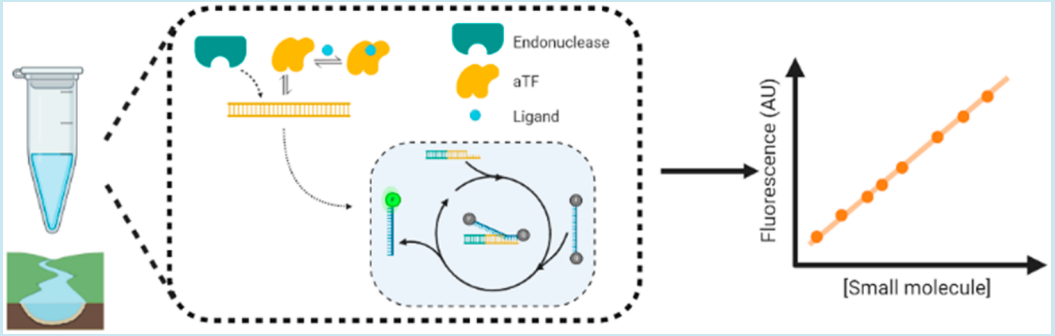

ABSTRACT: Detection of environmental pollutants is crucial to safeguard ecological and public health. Here, we report a modular biosensing approach for the detection of contaminants based on the regulation of a minimal DNA signal amplifier and transducer circuit by allosteric transcription factors and their cognate ligands. We leverage the competition between allosteric proteins and an endonuclease to modulate cascade toehold-mediated strand displacement reactions, which are triggered in the presence of specific effectors and sustained by the endonuclease. We built two optical biosensors for the detection of tetracyclines and macrolides in water using repressors TetR and MphR, respectively. We demonstrate that our minimal, fast, and single-step biosensors can successfully detect antibiotics in nanomolar levels and apply them to report the presence of spiked-in antibiotics in water samples in a matter of minutes, suggesting great potential for monitoring of water contaminants.

KEYWORDS: *small molecule biosensor, transcription factor, antibiotic detection, toehold-mediated strand displacement*

Monitoring of small molecules in the environment has become crucial to safeguard human and environmental health. Antibiotics, metals, and other pollutants have been found in water bodies all around the world as a consequence of anthropogenic emission and geological sources.[1−4] Unfortunately, conventional analytical methods like high performance liquid chromatography (HPLC) and mass spectrometry (MS)[5,6] are not scalable enough to cover the demand for water monitoring in most affected areas, due to costly equipment and infrastructure, logistic challenges that involve sample transportation and storage, and the need of skilled personnel to perform the analysis and interpret the results.

Biosensors are a viable alternative for detection of many water pollutants, ideally being easy-to-use and field-deployable, and requiring little to no energy to function.[7−9] Among different sensor biomolecules, allosteric transcription factors (aTFs) are used to build biosensing circuits orchestrated by protein−ligand−nucleic acid interactions to sense specific analytes, such as small molecules, and trigger signal transduction reactions that output measurable optical or electrochemical signals.[10,11] The growing characterization and engineering of aTFs hold great potential for the development of biosensing platforms for a variety of cognate chemicals.[12−14] Over the years, many aTF-based biosensors have been reported using aTFs with different signal transduction and amplification strategies, such as qPCR, loop-mediated isothermal amplification (LAMP), recombinase polymerase amplification (RPA), CRISPR-Cas12/13 systems, in vitro transcription, and so forth.[15−19] However, many of these approaches still require multiple preparation or preincubation steps, temperature cycling, long turnaround time (>100 min), conjugation and protein immobilization/modification, complex formulation, low sensitivity, and high variability, among others.

Our goal was to build a simple, fast, single-step biomolecular circuit to transduce and amplify aTF-ligand binding events. Dynamic nucleic acid strand displacement reactions are well suited for simple and thermodynamically controlled circuits.[20−24] In toehold-mediated strand displacement (TMSD)

Received: October 26, 2020
Published: January 22, 2021

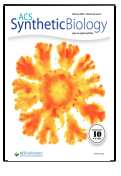

Scheme 1. Design of the Biosensor[a]

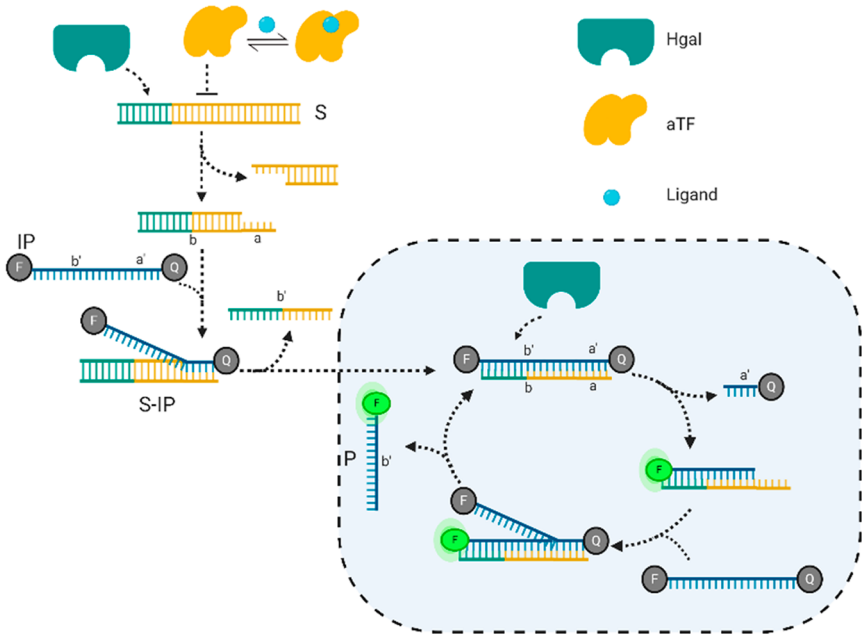

[a]An aTF and the restriction enzyme HgaI allosterically regulate cycling toehold-mediated strand displacement reactions enabled by HgaI cleavage. In the signal amplification stage (blue rectangle), the DNA template (S) is recycled, and a fluorescent signal is generated through continuous cleavage of a labeled invading probe (IP) sustained by strand displacement. The minimal and modular design of the biosensor enables one-pot, fast detection of ligands. S, DNA template; IP, Invading Probe; S-IP, DNA template/IP intermediary; aTF, allosteric transcription factor. a and b indicate different DNA domains, and (′) indicates complementarity.

reactions, an oligonucleotide binds to a toehold (a dangling single-stranded region of a dsDNA) and triggers a branch migration step, resulting in the displacement and dissociation of the strand originally hybridized in the double-stranded substrate.[25,26] However, one condition for toehold exchange reactions to sustain is the repetitive interaction between target and probe oligonucleotides to thermodynamically drive the reaction through exposure and sequestration of toehold domains. Therefore, the activation of DNA circuits, with a few exceptions,[27,28] relies mostly on nucleic acid inputs.

In this study, we report a signal transduction and amplification mechanism based on TMSD reactions that is actuated by small molecules via the allosteric regulation of ligand-responsive transcription factors. The allostery of transcription repressors regulates the kinetics of toehold-mediated strand displacement reactions and enables minimal, rapid, and programmable optical biosensors. Their utility and modularity were demonstrated by detecting antibiotics from two different families in environmental water samples using specific aTFs.

RESULTS

Biosensor Principle and Design. Toehold-mediated reactions for signal amplification mechanisms rely on the interaction between oligonucleotide target and probes at different toehold domains. Hence, the first step in our design was to trigger the generation of a toehold domain in a DNA template induced by a ligand input. For this, we leveraged the competition between an aTF and a restriction enzyme for the same DNA template to regulate the activity of the latter. In Scheme 1, the restriction enzyme HgaI competes with an aTF for the operator sequence in a double-stranded DNA template (S), which contains the HgaI recognition site (HRS) upstream of the operator. When the cognate effector (Ligand) is absent, the aTF binds to the operator and protects it from HgaI cleavage. Conversely, the formation of the aTF/ligand complex allows HgaI to bind and cleave S, leaving a product with a 5-nucleotide-long overhang on the 3′. This toehold domain (a) acts as the nucleation site for an invading strand (IP) that contains a fluorophore/quencher pair and results in the displacement of the short strand of S (b′). The new dsDNA fragment (S-IP) enters a cycle of continuous cleavage by HgaI and regeneration by IP, resulting in the accumulation of a displaced fluorescent strand (P). Thus, the presence of a specific ligand is visualized as an increase in the fluorescent signal.

The strength of toehold-mediated strand displacement is driven by the toehold length, where a toehold of five or more nucleotides yields a maximum reaction rate of $\sim 1 \times 10^6$ M^{-1} s^{-1}.[26] Hence, a mechanism that generates an overhang of this length would make the reaction possible. HgaI is a type II restriction enzyme that recognizes asymmetric DNA sequences and cleaves outside of its recognition site. This is desirable because it allows the design of DNA templates with different operator sequences specific to other aTFs.

aTFs Can Regulate Toehold-Mediated Strand Displacement Reactions. We first investigated whether an aTF could protect the DNA template from HgaI cleavage. We chose the well-characterized tetracycline repressor and its operator, TetR and tetO, respectively. Tetracyclines are widely used in agriculture and farming, and their detection in water and soil is urgently needed.[29] We used the electromobility shift assay (EMSA) to confirm that TetR binds to the DNA template containing tetO and releases it in the presence of tetracycline (SI Figure S1a). Next, we evaluated the effect of spacing between the HgaI recognition site and tetO using templates that contained 2, 4, 6, 8, 10, and 12 bp spacers

https://dx.doi.org/10.1021/acssynbio.0c00545
ACS Synth. Biol. 2021, 10, 371−378

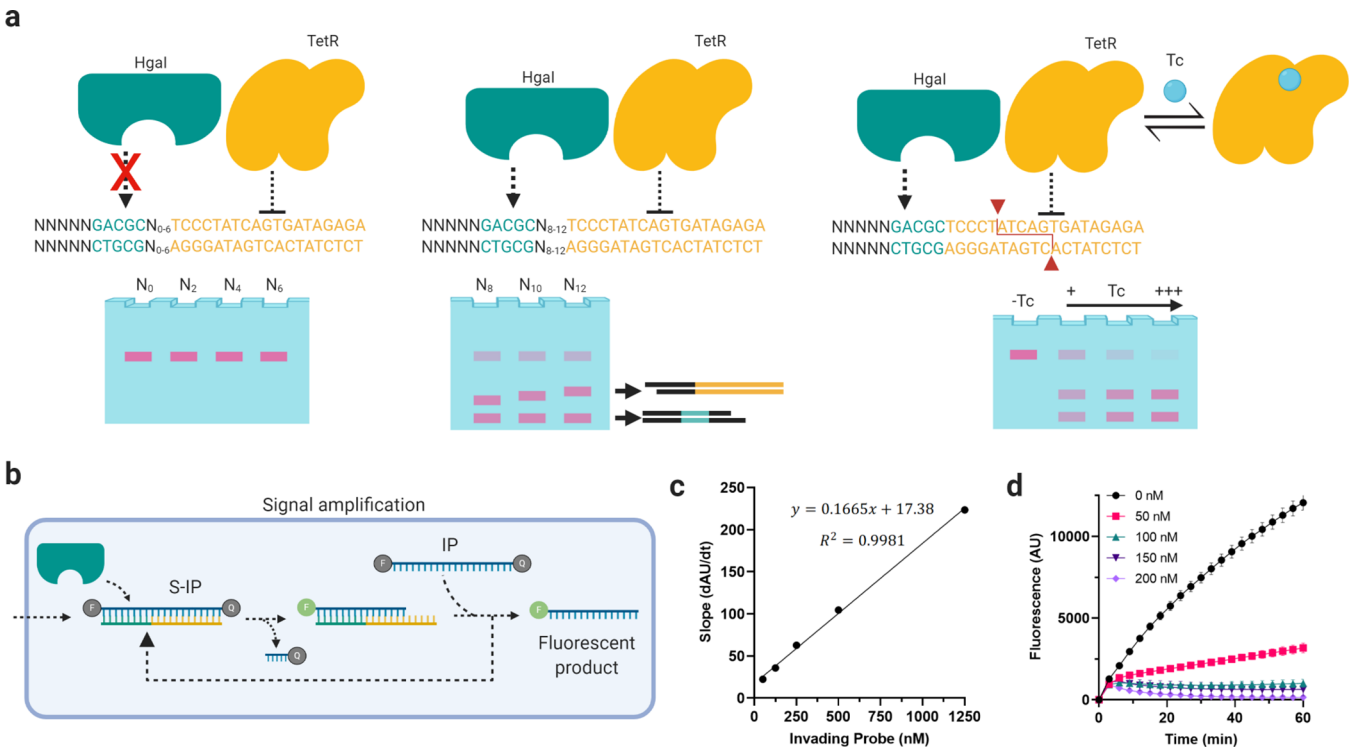

Figure 1. Regulation of TMSD by allosteric Transcription Factors. (a) Illustration of the effect of 2*X*-bp spacers (N_{bp}, X = 0−6) on the protection of the DNA by TetR from HgaI cleavage and its regulation upon addition of tetracycline (Tc). Complete PAGE results can be found in Supporting Information (SI) Figure S1b,c. (b) Illustration of signal amplification stage enabled by constant cleavage and regeneration of a quenched DNA fluorescent substrate. (c) Linear relationship between the Invading Probe concentration and the cleavage rate (fluorescence slope). DNA template = 50 nM. (d) Decrease in the fluorescence intensity as a result of TMSD repression by different concentrations of TetR. DNA template = 50 nM, IP = 1.25 μM. Symbols indicate mean values and error bars indicate s.d. n = 3 (c,d).

(N_{0-12}). We incubated each of the templates with TetR and HgaI for 30 min at 37 °C prior digestion of the proteins with proteinase K and used polyacrylamide gel electrophoresis (PAGE) to view the cleaved products. We observed that DNA containing 0−6 bp spacers showed one band in PAGE, suggesting that TetR can protect the DNA from cleavage when the operator sequence is located up to 6 bp downstream of the HgaI recognition site. Spacers longer than 6 bp did not protect the DNA from HgaI cleavage and are shown as two shorter bands in PAGE. Therefore, we decided to position the HRS immediately upstream (N_0). Finally, we observed allosteric control of cleavage upon addition of tetracycline to protected DNA (DNA/TetR complex), which resulted in shorter bands observed in PAGE (Figure 1a, SI Figure S1b,c).

Next, we sought to corroborate that the toehold-mediated strand displacement reactions were occurring as shown in Figure 1b. We set up reactions containing the DNA template (S), HgaI, and different ratios of invading probe (IP) over S ranging from 1-fold (1×) to 25-fold (25×). As expected, increasing concentrations of IP resulted in higher accumulation of the displaced fluorescent product (P). We observed that the slope of the fluorescence intensity showed a good linear relationship (R^2 = 0.9981) with the concentration of IP in the first 5−30 min of reaction (Figure 1c; SI Figure S2a,b). In this time frame, 2.5×, 5×, 10×, and 25× were 1.6, 2.8, 4.7, and 10 times, respectively, faster than the equimolar reaction (1×). Hence, we chose 25-fold excess over S for future reactions.

In our strategy, the sensitivity is directly related to the concentration of aTF. This is because any excess of aTF will act as a ligand chelator and desensitize the sensor, as demonstrated by Lucks' group to shift the sensitivity of a copper sensor using aTF-regulated in vitro transcription reactions.[19] Because of thermodynamic equilibrium, if the concentration of the transcription factor is reduced, the DNA template would need to be lowered accordingly maintaining the stoichiometry. At the same time, the concentration of DNA would need to be enough to trigger the TMSD reactions, so we chose 50 nM as the minimum concentration of DNA (SI Figure S2c).

We then validated that the blockage of HgaI by TetR observed in PAGE was applicable to the full TMSD reaction. Based on the EMSA results that confirmed the allostery of TetR (SI Figure S1a), different excesses of TetR ranging from 1× to 4× were added to TMSD reactions. We observed an increase in fluorescence during the first 5 min for all the reactions, which we believe is the time required for the stabilization and possibly nonspecific interactions. Hence, we took the 5 min mark as the start of the reactions. We found that 2-fold excess of TetR was enough to repress the overall reaction and kept the fluorescence intensity at practically zero over 60 min (Figure 1d; SI Figure S3).

To support the results of the repression and further expand the range of small molecules that can be sensed, we applied the same strategy using MphR and mphO, which are a macrolide-responsive transcriptional repressor and its operator sequence, respectively. The reduction in the fluorescence rate and intensity as the concentration of MphR increased was confirmed (SI Figure S4). However, to repress the reaction by ∼90%, a significantly higher concentration of MphR was needed, compared to TetR (3 μM and 100 nM, respectively).

https://dx.doi.org/10.1021/acssynbio.0c00545
ACS Synth. Biol. 2021, 10, 371−378

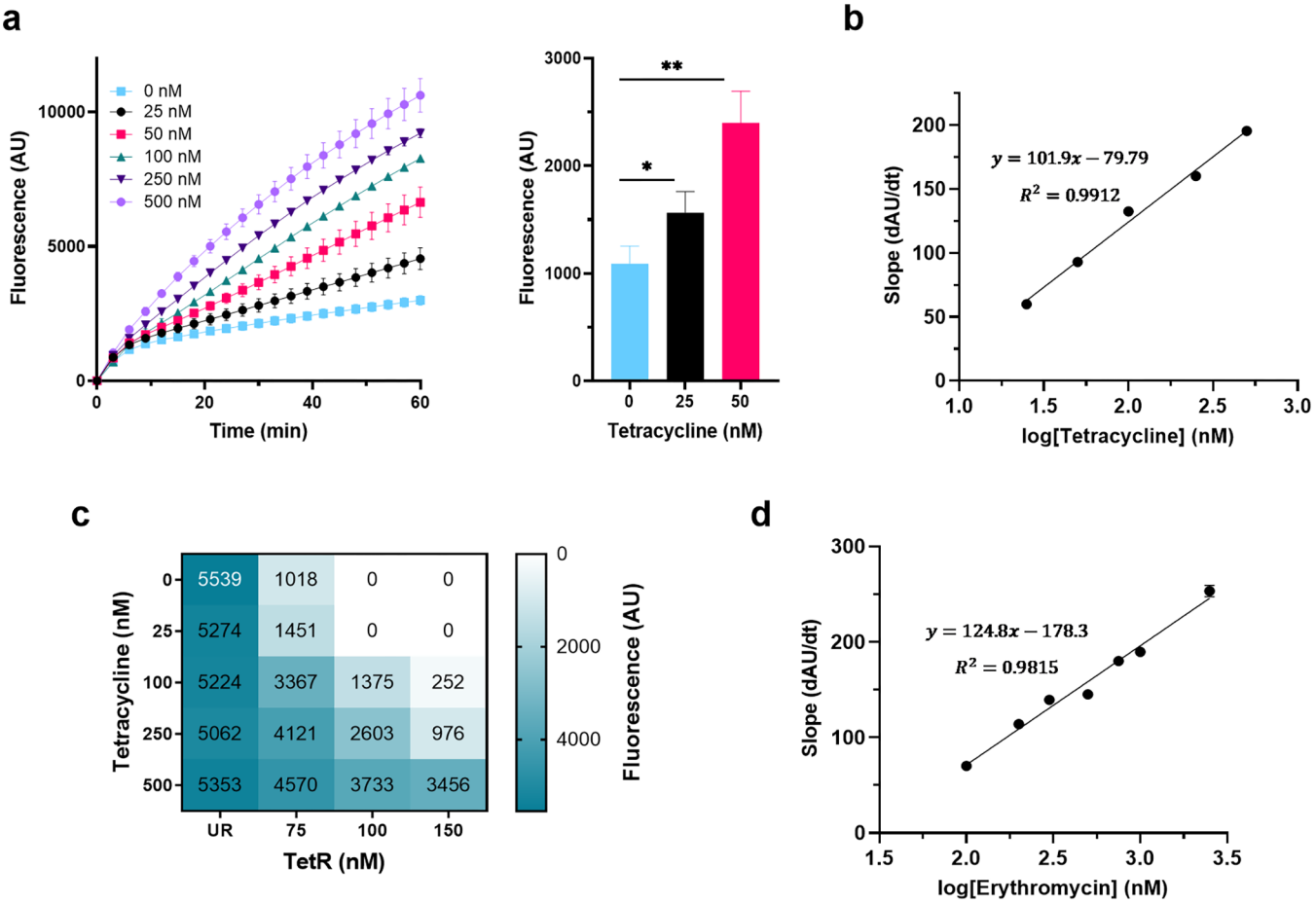

Figure 2. Activation of TMSD signal amplification reactions by small molecules. (a) Fluorescence intensity of induction at a range of tetracycline concentrations (*p-value <0.05; **p-value <0.005 using a two-tailed t test; data taken at 20 min with the 5 min mark as the starting point). DNA template = 50 nM, TetR = 75 nM. (b) Linear relationship between fluorescence rate and tetracycline concentration in the 25−500 nM range. (c) Fine tuning of tetracycline biosensor. End-point (at 20 min) fluorescence intensity of biosensors repressed over a range of TetR concentrations (150 nM to UR: 0 nM, unrepressed) induced by tetracycline 0−500 nM. Values represent the average AU of fluorescence of 2 independent replicates. (d) Linear relationship between fluorescence rate and erythromycin concentration in the 100−2500 nM range. DNA template = 50 nM, MphR = 3 μM. All the stated concentrations of ligands are sample concentrations. Final ligand concentrations correspond to half of the indicated in each figure. Symbols and bars indicate mean values and error bars indicate s.d. n = 3 (a, b, d); n = 2 (c).

This was expected as the dissociation constant (K_d) of MphR and its operator is 3 orders of magnitude higher than that of TetR/tetO (574 nM vs 0.2 nM).[30,31] Interestingly, the kinetics of all reactions remained with a linear behavior with slope approximating zero as the fold-excess of aTF increased.

Allosteric Regulation of TMSD Enables Small Molecule Detection. Knowing that the fluorescence rate depends on the amount of free DNA template, we did simulations of the DNA−aTF-ligand interactions to evaluate the repression and induction of the reactions with aTFs and ligand, respectively (SI Note S1, SI Figure S5). As seen on the mathematical model, increasing concentrations of ligand with fixed concentrations of repressor result in more free DNA template to be recycled in TMSD reactions and behaves as a characteristic ligand-binding curve. Thus, as the rate of the target-recycling TMSD reactions is proportional to the concentration of DNA template, we would expect the fluorescence intensity rate of the induced reactions to behave like the curves obtained.

We next induced the de-repression of TMSD reactions with the aTFs' cognate ligands. We performed the reactions over a range of concentrations of tetracycline in systems containing 75 nM of TetR and 50 nM of DNA template. Fluorescence intensity followed consistent linear kinetics in the first 5−30 min with increasing slopes as the concentration of tetracycline increased (Figure 2a, SI Figure S6a). The fluorescence activation response followed a qualitative trend as in the model, and the slope of the fluorescence intensity showed a linear relationship (R^2 = 0.9912) with increasing concentrations of the target in the range of 25−500 nM (Figure 2b, SI Figure S6).

For some applications, detection of contaminants such as arsenic, copper, or lead (for which there are known aTFs) can be simplified to litmus-type biosensors with known thresholds or "safe limits" determined by institutions like USEPA and WHO.[32,33] In such cases, we can tune the biosensor to trigger the signal amplification cycle at higher analyte concentrations by increasing the concentration of the repressor. In our results, although we could detect as low as 25 nM of tetracycline, repression with 75 nM of TetR resulted in only partially repressed reactions and significantly reduced the fold-change between negative and induced reactions. We induced the biosensors, repressed with varying concentrations of the TetR repressor, with a range of tetracycline concentrations to

https://dx.doi.org/10.1021/acssynbio.0c00545
ACS Synth. Biol. 2021, 10, 371−378

evaluate their sensitivity. Increasing concentrations of TetR shifted the biosensor's sensitivity to higher concentrations of tetracycline. For example, using 100 nM of repressor could no longer trigger TMSD upon induction with 25 nM of tetracycline. Similarly, fluorescence activation by 100 nM of the ligand is virtually negligible when the biosensor is repressed with TetR 150 nM. Importantly, both cases resulted in null fluorescence in the absence of the ligand (Figure 2c). We believe this allows a clearer readout, can avoid potential false positives, and ensures a more robust detection by increasing the fold-change between repressed and induced conditions, which is desired for further adaptation of the system in field-deployable strategies. It is noted, however, that desensitizing the biosensor with high fold-excess of repressor over DNA template could result in slower reactions due to lower free DNA in equilibrium even at high concentrations of ligands as observed in the mathematical model. This effect might be counteracted by using a higher concentration of DNA and a fold-excess of repressor that can still fully repress the reaction (SI Figure S5c). However, further analysis and experimental work are necessary to investigate whether the scenarios of small molecules with different dissociation constants would follow this prediction.

Finally, when using MphR and its corresponding DNA template and Invading Probe, as little as 100 nM of erythromycin could be detected. Similarly, the reaction rate had a linear relationship in the range of 100−2500 nM of the analyte (Figure 2d, SI Figure S7).

In all scenarios, we observed that though the fluorescent signal increases proportionally to the analyte, it does not reach the rate and intensity of unrepressed reactions as there is always a fraction of DNA bound with aTF due to thermodynamic constraints even at high ligand concentration (SI Figure S5a,b). Altogether, these results indicate that allosterically regulated TMSD reactions can be used as biosensors, allowing optical readouts in a ligand concentration-dependent manner within 5 to 30 min.

Detection of Antibiotics in Environmental Samples. To test the applicability of the biosensors, we used environmental matrices. We collected water samples from a pond in Hong Kong and performed the reactions with these instead of laboratory-grade water (Milli-Q). First, we evaluated the effect of the filtered samples (0.45 μm syringe-filter) on unrepressed and repressed TMSD reactions. We observed that the unrepressed reactions occurred as expected but with a reduction in fluorescence. Importantly, repressed reactions with their corresponding aTF resulted in similar kinetics and final fluorescent intensity slightly lower than of those with lab-grade water (SI Figure S8). Later, we confirmed that biosensors are only activated by their cognate ligands spiked in water samples, showing no crosstalk with other antibiotics (Figure 3).

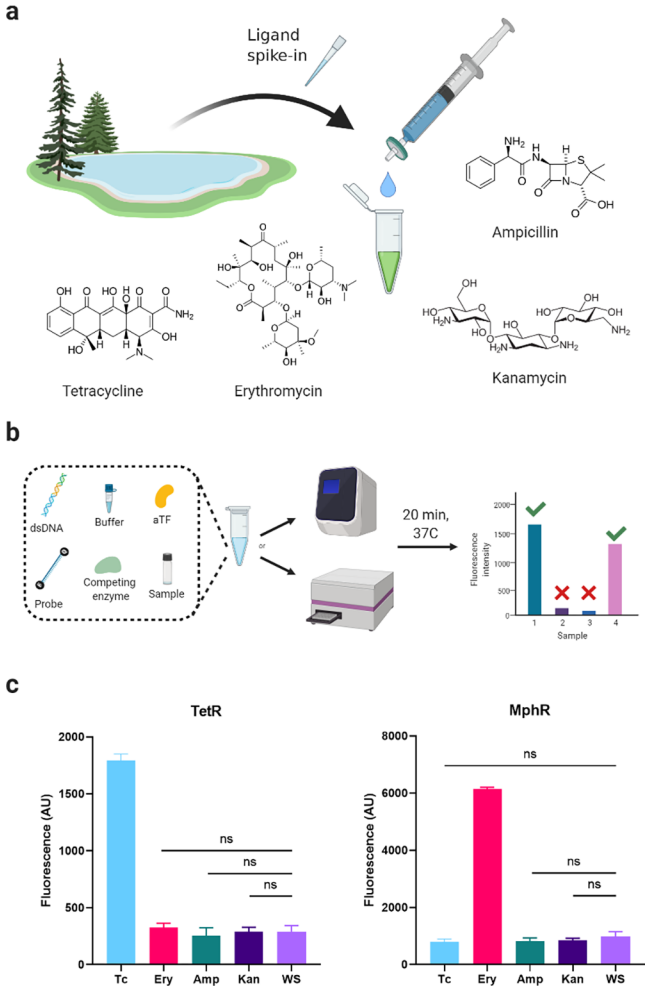

Figure 3. Test of the biosensors with environmental matrices. (A) Environmental samples were taken at a pond in Hong Kong. After collection, samples were spiked with different antibiotics (where applicable) and immediately filtered using a syringe-filter. (B) The overall workflow from sample filtration to result can be accomplished within 25 min. (C) The sensors successfully reported the presence of spiked-in antibiotics in water samples with no crosstalk. 500 nM aliquots of each ligand were used for the TetR-based biosensors (250 nM final concentration). 2.5 μM aliquots of each ligand were used for the MphR-based biosensors (1.25 μM final concentration). (ns: p-value >0.05 between noncognate ligand and WS using a two-tailed t test). Tc = Tetracycline, Ery = Erythromycin, Amp = Ampicillin, Kan = Kanamycin, WS = Water Sample (no analyte). Bars indicate mean values, and error bars indicate s.d. n = 2 (c).

DISCUSSION

Traditional DNA-based molecular circuits have mostly relied on RNA/DNA triggers. In this study, we demonstrated the modular and programmable actuation of a simple DNA circuit by small molecules, leveraging the specificity of allosteric transcription factors for cognate ligands and the modularity of enzyme-enabled toehold mediated strand displacement reactions. By allosterically controlling a signal amplification cycle of DNA cleavage and strand displacement, we built two optical biosensors that respond to tetracycline and erythromycin. The results reported here support the usefulness of our biosensors to detect small molecules in environmental samples from surface waters with only minimal pretreatment.

The biosensors presented here suggest the possibility to adapt a minimal, fast, affordable, and single-step strategy to other aTFs/ligands. Leveraging the modularity and specificity of DNA reactions, we anticipate that multiplexed sensors can be built and tuned to detect many targets at different thresholds. Nevertheless, a few limitations of the method arise. We observed that aTF/DNA binding is affected in different conditions (data not shown). Buffer composition and ion concentrations are factors that directly affect dissociation constants between aTFs, DNA, and ligands, which could impact the sensitivity and rate of the reactions because of changes in the amount of free DNA in equilibrium. Optimizing

https://dx.doi.org/10.1021/acssynbio.0c00545
ACS Synth. Biol. 2021, 10, 371−378

the reaction composition, using a different restriction enzyme that operates in a more suitable buffer, or even utilizing engineered aTFs with improved binding are some of the alternatives to these limitations.

We observed a reduction in the fluorescence signal when detecting antibiotics in spiked environmental water samples. This suggests that more complex matrices may have a larger negative effect on the reactions, through inhibition of the enzyme activity or fluorescence quenching. While only filtering the water with a 0.45 μM syringe filter was sufficient for water samples, samples with different physical and chemical properties (wastewater, soil, drinks, etc.) may require more sophisticated sample preparation methods, such as solid-phase extraction. In cases where the "safe limit" of the analyte and sensitivity of the biosensor allows, dilution could be a simple alternative to decrease matrix effects.

Investigation into preservation techniques such as freeze–drying could potentially enable the deployment of these biosensors in the field,[34] using different instruments such as hand-held or smartphone-based fluorometers, or other colorimetric readouts.[35−37] The ∼6-fold increase in fluorescence signal using environmental samples is comparable to recently reported water contaminant biosensors.[19] However, the signal intensity obtained after 20 min of reaction might be too low for visualization with the naked eye using simple portable devices such as an illuminator. Portable devices with specific components such as a photodiode, a heating element, and a design that blocks external light for reliable detection would be more suitable for field deployment. Many reported prototypes could be adapted for this application using inexpensive off-the-shelf components, 3-D printing, and open-source software,[37,38] with the potential to expand the capabilities of the biosensor to quantitative detection. Moreover, we believe that our strategy can be deployed using other formats, such as lateral flow assays, with minimal modification of the invading probe.

Overall, this work demonstrates a novel actuation mechanism of DNA-based circuits applied to modular, simple, and fast detection of small molecules. Further development and integration of different technologies into consolidated platforms is key to leveraging the potential of DNA reactions to sense and report the presence of non-nucleic acid targets in the environment.

METHODS

Strain and Growth Medium. *E. coli* BL21 DE3 (Sangon, China) was used for recombinant protein expression. The growth media used was Lysogeny (LB) agar or broth supplemented with kanamycin (Thermo Fisher Scientific #J17924) (50 ug/mL).

Plasmid and DNA Parts. pET-28a plasmids encoding aTFs were ordered directly from Sangon Biotech. They were designed to express the proteins with a C-terminus His-tag (SI Table S1). DNA oligonucleotides to form the dsDNA sensor and DNA fluorescent probes (5′6-FAM−3′BHQ1) were ordered from Integrated DNA Technologies (SI Table S1). The complementary oligonucleotides were annealed in Tris-EDTA (TE) buffer pH 7.5, 12.5 mM $MgCl_2$ with a final concentration of 10 μM of dsDNA using a thermocycler (95 °C 5 min, −0.5 °C/min, 20 °C 10 min). Dilutions to final working concentrations were made accordingly with TE buffer pH 7.5.

aTF Expression and Purification. Streak-plating onto LB Agar supplemented with kanamycin was used to pick single colonies of *E. coli* BL21 DE3 containing pET-28a. A single colony was used to grow a 10 mL overnight culture at 200 rpm and 37 °C, and this subsequently a 500 mL culture. At OD600 of 0.5, the culture was induced with 250 μM IPTG (Sigma-Aldrich #I6758) and grown for 5 h in the same conditions. Cell pellet was recovered after centrifugation at 4000 rpm for 20 min and resuspended in lysis buffer (PBS pH 7.4 (Thermo Fisher Scientific #28372), 1× Halt Protease Inhibitor (Thermo Fisher Scientific #1861278), 10 mM Imidazole) or kept at −20 °C for a maximum of 7 days in PBS pH 7.4. The suspension was ultrasonicated on ice (5 cycles of 1 min with 1 min of rest, 50% duty cycle) and centrifuged at 13,000*g* for 30 min. The supernatant was then used to purify the His-Tagged proteins using Ni-NTA agarose (Qiagen # 30210) in gravity column (10 mM, 25 mM, and 250 mM imidazole in PBS for equilibration, washing, and elution, respectively). Centrifugal filters (Amicon Ultra 4, Millipore) were used to desalt (final buffer was PBS) and concentrate the purified protein. Confirmation of the purification was carried out by reducing SDS-PAGE 12% (SI Figure S9) and concentration determination by Bradford Assay. Proteins were kept at −20 in 50% glycerol, and dilutions were made accordingly with PBS.

Gel Electrophoresis and Electrophoretic Mobility Shift Assay. PAGE 12% (room temperature at 90 V in TBE 1× buffer) was used to visualize the activity of HgaI on DNA templates with spacers of different length (SI Figure S1b). Reactions containing DNA template, TetR, and HgaI were incubated at 37 °C and stopped after 30 min by addition of Proteinase K (New England Biolabs #P8107S) and incubation for 10 additional minutes. This step was to stop HgaI and release any noncleaved DNA from TetR. PAGE 12% under the same conditions was also used to show the products of TMSD reaction (SI Figure S2).

To evaluate the allostery of the TetR (SI Figure S1a,c) dsDNA was mixed with the different ratios of the aTF and equilibrated in NEBuffer 1.1 (New England Biolabs #B7201S) at room temperature. EMSA was carried out on PAGE 10% at room temperature at 90 V in TBE 1× buffer. Post staining was done with SYBRGold (Thermo Fisher Scientific #S11494) 1× in TBE 1× buffer.

Reaction compositions are as described in the corresponding figures, and all were performed using final concentration of 1× NEBuffer 1.1 (New England Biolabs #B7201S), unless indicated otherwise.

HgaI/Toehold-Mediated Strand Displacement Reactions. Reactions were set up by adding Buffer 1.1 (New England Biolabs), dsDNA template, invading strand, aTF, nuclease-free water (Integrated DNA Technologies) or sample, and HgaI (New England Biolabs), to a final volume of 10 uL. Immediately after adding HgaI, 6-FAM fluorescence intensity was monitored over 30−120 min on a CFX96 Touch Real Time PCR Detection System (BioRad) on Channel 1. Detailed formulation of HgaI restriction reactions can be found in SI Table S2.

Water Sampling and Processing. Water samples were taken from a pond in eastern Hong Kong (22.332022, 114.245774). Samples were collected in sterile 50 mL Falcon tubes and transported to the lab at room temperature (1 h). In the lab, they were filtered using a 0.45 μm syringe filter and immediately used for the reactions. Corresponding samples were spiked with known concentrations of tetracycline (Sigma-

https://dx.doi.org/10.1021/acssynbio.0c00545
ACS Synth. Biol. 2021, 10, 371−378

Aldrich #87128), erythromycin (Sangon Biotech CAS#114−07−8), kanamycin (Thermo Fisher Scientific #J17924), or ampicillin (Sigma-Aldrich #A9518) prior to filtering. All reactions using water samples (spiked or not) were performed on the day of collection, with a maximum of 2 h between collection and reaction. For data shown in Figure 3, 500 nM (final concentration 250 nM) antibiotics was used to test the TetR-based biosensor, and 2.5 μM (final concentration 1.25 nM) was used with the MphR-based biosensor. 50 nM of DNA template and 1.25 μM of Invading Probe were used in all reactions (SI Figure S8 and Figure 3).

Data Processing and Visualization. All raw data was processed and analyzed with Microsoft Excel and GraphPad Prism 8. All graphs were generated with GraphPad 8 and Matlab. Schemes and illustrations were created with Biorender.com.

■ ASSOCIATED CONTENT

Supporting Information

The Supporting Information is available free of charge at https://pubs.acs.org/doi/10.1021/acssynbio.0c00545.

Figures S1−S8 including PAGE and EMSA results of allosteric mediation of HgaI cleavage and signal amplification reaction, plots showing signal amplification kinetics; plots showing reaction repression by TetR and MphR; simulation results of free DNA in different concentrations of repressor, inducer and template DNA; dose−response curves of tetracycline and macrolides biosensors; effect of water samples on the biosensors performance; SDS-PAGE of purified repressors. Note S1 describing the mathematical model for free DNA estimation. Tables S1−S2 with protein and DNA sequences used for biosensors construction. (PDF)

■ AUTHOR INFORMATION

Corresponding Author

I-Ming Hsing − *Department of Chemical and Biological Engineering, The Hong Kong University of Science and Technology, Kowloon, Hong Kong;* orcid.org/0000-0002-3326-3021; Email: kehsing@ust.hk

Author

Alan F. Rodríguez-Serrano − *Department of Chemical and Biological Engineering, The Hong Kong University of Science and Technology, Kowloon, Hong Kong;* orcid.org/0000-0003-1424-1246

Complete contact information is available at: https://pubs.acs.org/10.1021/acssynbio.0c00545

Author Contributions

All authors have given approval to the final version of the manuscript.

Notes

A.F.R.-S. and I.H have filed a provisional patent application in the field of in vitro small molecule biosensing.

The authors declare no competing financial interest.

■ ACKNOWLEDGMENTS

A.F.R.-S. would like to thank the Hong Kong Ph.D. Fellowship Scheme from Hong Kong SAR Government and support from Conacyt-Mexico. Funding support from the Research Grants Council of Hong Kong SAR Government (Project Nos. GRF# 16301817 and GRF# 16306218) is acknowledged. The authors acknowledge the use of Biorender.com for the creation of all schemes, illustrations, and the TOC graphic.

■ REFERENCES

(1) Damania, R., Desbureaux, S., Rodella, A.-S., Russ, J., and Zaveri, E. (2019) Quality Unknown: The Invisible Water Crisis, in *Quality Unknown: The Invisible Water Crisis*, p 66, The World Bank.

(2) Dada, E. O., and Ikeh, R. K. (2018) Phthalate and metal concentrations in drinking water in Lagos, Nigeria. *J. Heal. Pollut. 8*, 180603.

(3) Rosso, J. J., Schenone, N. F., Pérez Carrera, A., and Fernández Cirelli, A. (2013) Concentration of arsenic in water, sediments and fish species from naturally contaminated rivers. *Environ. Geochem. Health 35*, 201−214.

(4) Gothwal, R., and Shashidhar, T. (2015) Antibiotic Pollution in the Environment: A Review. *Clean: Soil, Air, Water 43*, 479−489.

(5) Gavilán, R. E., Nebot, C., Veiga-Gómez, M., Roca-Saavedra, P., Belda, B. V., Franco, C. M., and Cepeda, A. (2016) A Confirmatory Method Based on HPLC-MS/MS for the Detection and Quantification of Residue of Tetracyclines in Nonmedicated Feed. *J. Anal. Methods Chem. 2016*, 1202954.

(6) Rosen, R. (2007) Mass spectrometry for monitoring micropollutants in water. *Curr. Opin. Biotechnol. 18*, 246−251.

(7) Thavarajah, W., Verosloff, M. S., Jung, J. K., Alam, K. K., Miller, J. D., Jewett, M. C., Young, S. L., and Lucks, J. B. (2020) A primer on emerging field-deployable synthetic biology tools for global water quality monitoring. *npj Clean Water 3*, 18.

(8) McConnell, E. M., Nguyen, J., and Li, Y. (2020) Aptamer-Based Biosensors for Environmental Monitoring. *Front. Chem. 8*, 434.

(9) Justino, C. I. L., Duarte, A. C., and Rocha-Santos, T. A. P. (2017) Recent progress in biosensors for environmental monitoring: A review. *Sensors 17*, 2918.

(10) Fernandez-López, R., Ruiz, R., de la Cruz, F., and Moncalián, G. (2015) Transcription factor-based biosensors enlightened by the analyte. *Front. Microbiol. 6*, 648.

(11) Silverman, A. D., Akova, U., Alam, K. K., Jewett, M. C., and Lucks, J. B. (2020) Design and Optimization of a Cell-Free Atrazine Biosensor. *ACS Synth. Biol. 9*, 671−677.

(12) Taylor, N. D., Garruss, A. S., Moretti, R., Chan, S., Arbing, M. A., Cascio, D., Rogers, J. K., Isaacs, F. J., Kosuri, S., Baker, D., Fields, S., Church, G. M., and Raman, S. (2016) Engineering an allosteric transcription factor to respond to new ligands. *Nat. Methods 13*, 177−183.

(13) Cuthbertson, L., and Nodwell, J. R. (2013) The TetR Family of Regulators. *Microbiol. Mol. Biol. Rev. 77*, 440−475.

(14) Hobman, J. L., Wilkie, J., and Brown, N. L. (2005) A design for life: Prokaryotic metal-binding MerR family regulators. *BioMetals 18*, 429−436.

(15) Cao, J., Yao, Y., Fan, K., Tan, G., Xiang, W., Xia, X., Li, S., Wang, W., and Zhang, L. (2018) Harnessing a previously unidentified capability of bacterial allosteric transcription factors for sensing diverse small molecules in vitro. *Sci. Adv. 4*, eaau4602.

(16) Iwasaki, R. S., and Batey, R. T. (2020) SPRINT: a Cas13a-based platform for detection of small molecules. *Nucleic Acids Res. 48*, e101.

(17) Liang, M., Li, Z., Wang, W., Liu, J., Liu, L., Zhu, G., Karthik, L., Wang, M., Wang, K. F., Wang, Z., Yu, J., Shuai, Y., Yu, J., Zhang, L., Yang, Z., Li, C., Zhang, Q., Shi, T., Zhou, L., Xie, F., Dai, H., Liu, X., Zhang, J., Liu, G., Zhuo, Y., Zhang, B., Liu, C., Li, S., Xia, X., Tong, Y., Liu, Y., Alterovitz, G., Tan, G. Y., and Zhang, L. X. (2019) A CRISPR-Cas12a-derived biosensing platform for the highly sensitive detection of diverse small molecules. *Nat. Commun. 10*, 3672.

(18) Nguyen, T. T., Chern, M., Baer, R. C., Galagan, J., and Dennis, A. M. (2020) A Förster Resonance Energy Transfer-Based Ratiometric Sensor with the Allosteric Transcription Factor TetR. *Small 16*, 1907522.

(19) Jung, J. K., Alam, K. K., Verosloff, M. S., Capdevila, D. A., Desmau, M., Clauer, P. R., Lee, J. W., Nguyen, P. Q., Pastén, P. A., Matiasek, S. J., Gaillard, J. F., Giedroc, D. P., Collins, J. J., and Lucks, J. B. (2020) Cell-free biosensors for rapid detection of water contaminants. *Nat. Biotechnol. 38*, 1451−1459.
(20) Chen, Y., Song, Y., Wu, F., Liu, W., Fu, B., Feng, B., and Zhou, X. (2015) A DNA logic gate based on strand displacement reaction and rolling circle amplification, responding to multiple low-abundance DNA fragment input signals, and its application in detecting miRNAs. *Chem. Commun. 51*, 6980−6983.
(21) Machinek, R. R. F., Ouldridge, T. E., Haley, N. E. C., Bath, J., and Turberfield, A. J. (2014) Programmable energy landscapes for kinetic control of DNA strand displacement. *Nat. Commun. 5*, 5324.
(22) Tang, W., Zhong, W., Tan, Y., Wang, G. A., Li, F., and Liu, Y. (2020) DNA Strand Displacement Reaction: A Powerful Tool for Discriminating Single Nucleotide Variants. *Top. Curr. Chem. 378*, 10.
(23) Zhang, Z., Fan, T. W., and Hsing, I. M. (2017) Integrating DNA strand displacement circuitry to the nonlinear hybridization chain reaction. *Nanoscale 9*, 2748−2754.
(24) Zhang, Z., and Hsing, I. M. (2017) Nucleic Acid Self-Assembly Circuitry Aided by Exonuclease III for Discrimination of Single Nucleotide Variants. *Anal. Chem. 89*, 12466−12471.
(25) Yurke, B., and Mills, A. P. (2003) Using DNA to power nanostructures. *Genet. Program. Evolvable Mach. 4*, 111−122.
(26) Zhang, D. Y., and Winfree, E. (2009) Control of DNA strand displacement kinetics using toehold exchange. *J. Am. Chem. Soc. 131*, 17303−17314.
(27) Vinkenborg, J. L., Karnowski, N., and Famulok, M. (2011) Aptamers for allosteric regulation. *Nat. Chem. Biol. 7*, 519−527.
(28) Engelen, W., Meijer, L. H. H., Somers, B., De Greef, T. F. A., and Merkx, M. (2017) Antibody-controlled actuation of DNA-based molecular circuits. *Nat. Commun. 8*, 14473.
(29) Scarano, C., Piras, F., Virdis, S., Ziino, G., Nuvoloni, R., Dalmasso, A., De Santis, E. P. L., and Spanu, C. (2018) Antibiotic resistance of Aeromonas ssp. strains isolated from Sparus aurata reared in Italian mariculture farms. *Int. J. Food Microbiol. 284*, 91−97.
(30) Cheng, Y., Yang, S., Jia, M., Zhao, L., Hou, C., You, X., Zhao, J., and Chen, A. (2016) Comparative study between macrolide regulatory proteins MphR(A) and MphR(E) in ligand identification and DNA binding based on the rapid in vitro detection system. *Anal. Bioanal. Chem. 408*, 1623−1631.
(31) Kamionka, A., Bogdanska-Urbaniak, J., Scholz, O., and Hillen, W. (2004) Two mutations in the tetracycline repressor change the inducer anhydrotetracycline to a corepressor. *Nucleic Acids Res. 32*, 842−847.
(32) Drinking Water Regulations. https://www.epa.gov/dwreginfo/drinking-water-regul.
(33) World Health Organization (2017) *Guidelines for Drinking-Water Quality: 4th Edition Incorporating the First Addendum.*
(34) Pardee, K. (2018) Perspective: Solidifying the impact of cell-free synthetic biology through lyophilization. *Biochem. Eng. J. 138*, 91−97.
(35) Chung, S., Breshears, L. E., Perea, S., Morrison, C. M., Betancourt, W. Q., Reynolds, K. A., and Yoon, J. Y. (2019) Smartphone-Based Paper Microfluidic Particulometry of Norovirus from Environmental Water Samples at the Single Copy Level. *ACS Omega 4*, 11180−11188.
(36) Morbioli, G. G., Mazzu-Nascimento, T., Stockton, A. M., and Carrilho, E. (2017) Technical aspects and challenges of colorimetric detection with microfluidic paper-based analytical devices (μPADs) - A review. *Anal. Chim. Acta 970*, 1−22.
(37) Alam, M. W., Wahid, K. A., Goel, R. K., and Lukong, K. E. (2019) Development of a low-cost and portable smart fluorometer for detecting breast cancer cells. *Biomed. Opt. Express 10*, 399.
(38) Nambannor Kunnath, R., Venukumar, A., and Gorthi, S. S. (2020) Handheld fluorometer for in-situ melamine detection via interference synthesis of dsDNA-templated copper nanoparticles. *Spectrochim. Acta, Part A 235*, 118304.

https://dx.doi.org/10.1021/acssynbio.0c00545
ACS Synth. Biol. 2021, 10, 371−378